

Research Article

Characterization and Expression of Senescence Marker in Prolonged Passages of Rat Bone Marrow-Derived Mesenchymal Stem Cells

Noridzzaida Ridzuan,^{1,2} Akram Al Abbar,³ Wai Kien Yip,⁴
Maryam Maqbool,^{1,2} and Rajesh Ramasamy^{1,2}

¹*Stem Cell & Immunity Group, Immunology Laboratory, Department of Pathology, Faculty of Medicine and Health Sciences, Universiti Putra Malaysia, 43400 Serdang, Malaysia*

²*Regenerative Medicine Research Program, Genetic and Regenerative Medicine Research Centre, Faculty of Medicine and Health Sciences, Universiti Putra Malaysia, 43400 Serdang, Malaysia*

³*Clinical Genetics Unit, Department of Obstetrics & Gynecology, Faculty of Medicine and Health Sciences, Universiti Putra Malaysia, 43400 Serdang, Malaysia*

⁴*Immunology Unit, Department of Pathology, Faculty of Medicine and Health Sciences, Universiti Putra Malaysia, 43400 Serdang, Malaysia*

Correspondence should be addressed to Rajesh Ramasamy; rajesh@upm.edu.my

Received 1 February 2016; Revised 23 May 2016; Accepted 23 May 2016

Academic Editor: Franca Fagioli

Copyright © 2016 Noridzzaida Ridzuan et al. This is an open access article distributed under the Creative Commons Attribution License, which permits unrestricted use, distribution, and reproduction in any medium, provided the original work is properly cited.

The present study is aimed at optimizing the *in vitro* culture protocol for generation of rat bone marrow- (BM-) derived mesenchymal stem cells (MSCs) and characterizing the culture-mediated cellular senescence. The initial phase of generation and characterization was conducted using the adherent cells from Sprague Dawley (SD) rat's BM via morphological analysis, growth kinetics, colony forming unit capacity, immunophenotyping, and mesodermal lineage differentiation. Mesenchymal stem cells were successfully generated and characterized as delineated by the expressions of CD90.1, CD44H, CD29, and CD71 and lack of CD11b/c and CD45 markers. Upon induction, rBM-MSCs differentiated into osteocytes and adipocytes and expressed osteocytes and adipocytes genes. However, a decline in cell growth was observed at passage 4 onwards and it was further deciphered through apoptosis, cell cycle, and senescence assays. Despite the enhanced cell viability at later passages (P4-5), the expression of senescence marker, β -galactosidase, was significantly increased at passage 5. Furthermore, the cell cycle analysis has confirmed the *in vitro* culture-mediated cellular senescence where cells were arrested at the G₀/G₁ phase of cell cycle. Although the currently optimized protocols had successfully yielded rBM-MSCs, the culture-mediated cellular senescence limits the growth of rBM-MSCs and its potential use in rat-based MSC research.

1. Introduction

Mesenchymal stem cells (MSCs) were originally isolated by Friedenstein and colleagues in guinea pig's bone marrow [1], characterized as multipotent adult stem cells that grow as foci with fibroblast-like morphology, termed as colony forming unit-fibroblasts (CFU-f). The early exploration and evaluation of MSC's biology were mainly achieved by exploiting bone marrow (BM) as a major source. To date, the common

and efficient source of MSCs is remained to be the bone marrow. Although the frequency of MSCs within the bone marrow is very low (0.001–0.1% of mononuclear cells), MSCs are capable of extensive proliferation and expansion at *in vitro* culture [2].

It is now recognized that MSCs reside in many tissues and organs other than bone marrow [3] such as adipose tissue [4], liver [5], skeletal muscle [6], umbilical cord [7], umbilical cord blood [8], placenta [9], and synovium [10]. Besides human,

TABLE 1: Basal media and FBS concentration used for CFU-f assay.

Basal media	FBS concentration (%)
Roswell Park Memorial Institute (RPMI) with GLUTAMAX-I	10
RPMI with GLUTAMAX-I	20
Dulbecco's Modified Eagle's Medium with nutrient mixture F12 (HAM) [1:1] DMEM/F12) with GLUTAMAX-I	10
DMEM/F12 with GLUTAMAX-I	20
Low glucose Dulbecco's Modified Eagle's Medium (LDMEM) with GLUTAMAX-I	10
LDMEM with GLUTAMAX-I	20
High glucose Dulbecco's Modified Eagle Medium (HDMEM) with GLUTAMAX-I	10
HDMEM with GLUTAMAX-I	20

MSCs have also been isolated from several animal species, namely, mouse [11–13], baboon [14], rat [15, 16], monkey [13], rabbit [17], dog [18], cat [19], and horse [20]. Despite the initial understanding on targeted/limited differentiation towards mesodermal lineages, the current studies have shown that, under a right stimulation, MSCs are able to differentiate into cells of endodermal and ectodermal origins such as β -pancreatic cells [21], hepatocyte [22], cardiomyocyte [23], skeletal muscle [24], neuron cells [25], and epithelial cells [26].

Many types of research that test the *in vivo* nature or functions of MSCs are still remarkably relying on animal models. Employing animals in biological science has become indispensable as most of the pharmacological and toxicological studies have been developed using laboratory-based animals as testing tools. For instance, the convenience of mice model with a possible genetic modification and availability of research reagents and species-specific antibodies ease the preclinical studies [27, 28]. Beside mouse model, some larger scale studies and disease-specific models were also developed using another type of animal such as rat, rabbit, fish, pig, and monkey [29–33]. In regard to current MSC research, human and mouse MSCs are extensively used in the present research scenario as these MSCs are relatively easy to be harvested and expanded in *in vitro* culture [34, 35]. When concerning other species, it has been reported that the rat MSCs are difficult to isolate and culture-expanded at the *in vitro* culture [15, 36, 37]. This conundrum drives the stem cells research using rat MSCs which is not as lucrative and well embraced as mouse counterpart. However, there is a need for the rat-based MSCs especially in diabetic research where most of the animal model investigations are tailored based on rats [38, 39]. One of the major concerns which arise in rat MSCs culture is to maintain a stable *in vitro* culture that provides an uninterrupted supply of stem cells for ongoing laboratory and animal works. Numerous research studies have reported the paucities of rBM-MS-C culture where after certain rounds of passages the cells were failed to be amplified at adequate numbers. Despite this observation, the exact mechanism of such growth retardation is not fully elucidated. Thus, this research project is aimed at optimizing the laboratory protocol for isolation, characterization, and expansion of rat MSC to fill the gap in the current rat-based MSCs studies.

2. Materials and Methods

2.1. Animals. Sprague Dawley (SD) rats (250–350 g and 5–8 weeks) were obtained from Chenur Supplier (Kajang, Selangor, Malaysia). Animals were acclimatized and handled with standard animal care procedures as prescribed by Institutional Animal Care and Use Committee, Universiti Putra Malaysia (IACUC, UPM). Animals were sacrificed by cervical dislocation.

2.2. Generation of Rat Bone Marrow MSCs. Bone marrow cells were obtained from Sprague Dawley (SD) rats by flushing femurs and tibiae and cultured in 25 cm² flask in a complete culture medium with 1% penicillin/streptomycin, 0.5% Fungizone, and 0.1% gentamycin (Gibco, United Kingdom). After 72 hours of plating, nonadherent cells were removed, and medium was replaced at every 48 hours. Adherent cells were further propagated and upon reaching 80–90% confluency, cells were trypsinised by using 0.05% trypsin-EDTA (Gibco, United Kingdom) at 37°C for 3–5 minutes. Harvested cells were cultured in 25 cm² flasks for further expansion. During expansion period, media were changed every 2 days. Expanded cells were either used for downstream experiments or cryopreserved using freezing media (10% DMSO and 90% FBS). Media used in rBM-MS-C expansion were LDMEM with GLUTAMAX-I (Gibco, United Kingdom), supplemented with 20% foetal bovine serum (FBS), 1% penicillin/streptomycin, 0.5% Fungizone, and 0.1% gentamycin (Gibco, United Kingdom). Supplements used in the optimization were 20 ng/mL basic fibroblast growth factor (bFGF) (R&D System USA), 1% nonessential amino acids (NEAA) (Gibco, United Kingdom), and 1% insulin transferrin sodium selenite (ITS) (Sigma Aldrich, USA).

2.3. Colony Forming Unit-Fibroblast Assay. Colony forming unit-fibroblast (CFU-f) assay was conducted with 1×10^6 of nucleated cells from freshly isolated rat bone marrow and seeded in 60 mm² cell culture dish (Becton Dickinson, USA) for 10 days. Various basal media were consumed to assess CFU-f as presented in Table 1 and purchased from Gibco, United Kingdom. Complete media were constituted with individual basal medium supplemented with 1% penicillin/streptomycin, 0.5% Fungizone, and 0.1% gentamycin.

TABLE 2: Primer sequence for adipocyte and osteocytes.

Primer	5'-3'	Sequence	Amplicon size	Annealing temperature (°C)
GAPDH	Forward	TGAACGGGAAGCTCACTGG	360	48.1
	Reverse	TCCACCACCCTGTTGCTGTA		
Osteopontin	Forward	CCGATGAATCTGATGAGTCCTT	303	57.8
	Reverse	TCCAGCTGACTTGACTCATGG		
Osteonectin	Forward	ATGAGGGCCTGGATCTTCTTTCTC	372	60.5
	Reverse	AAAGAAGTGGCAGGAAGAGTCGA		
PPAR γ	Forward	GCCTTGCTGTGGGGATGTCT	354	47.3
	Reverse	CGAAACTGGCACCCTTGAAAAAT		
C/EBPA	Forward	GCAGAAGGTGTTGGAGTTGA	214	66.7
	Reverse	AGCGACCCTAAACCATCCTC		

Media change was conducted every 2 days of interval. The cells were stained with 1.5% crystal violet (Sigma Aldrich, USA) in 100% methanol and incubated for 10 minutes. The number of colonies more than 2 mm was considered and counted.

2.4. Immunophenotyping. The expression of cell surface markers was measured by a direct immunofluorescence staining and analysed by flow cytometer. Cells at passages 2-3 were trypsinised and cell count was performed using trypan blue exclusion test. Upon staining, cells were transferred into Fluorescence Activated Cell Sorting (FACS) tubes and washed with 1x phosphate buffer saline (1xPBS). Cells were labelled with fluorochrome conjugated mouse anti-rat antibodies (CD90.1-PE, CD45-PE, CD11B/C-PE, CD29-FITC, CD71-FITC, and CD44H-FITC) for 15 minutes at 4°C. For analysis, 10,000 cells were acquired by LSR Fortessa flow cytometer (BD Biosciences, USA) and analysed using FACS Diva Software (BD Biosciences, USA).

2.5. Differentiation Assays. The adipocyte and osteogenic differentiation capabilities of passages 2-3 expanded rBM-MSCs were performed using StemPro adipogenesis differentiation kit (Gibco, Invitrogen, USA) and StemPro osteogenesis differentiation kit (Gibco, Invitrogen, USA), respectively, with minor modifications. Rat bone marrow mesenchymal stem cells were cultured in 60 mm² Petri dish and incubated at 37°C in 5% CO₂ humidified air. Upon reaching 100% confluency, cells were supplemented with respective differentiation medium where the inductive medium was changed every 2 days for 20 days. For adipogenic induction, cells were fixed in 4% paraformaldehyde and stained with Oil Red O solution whereas for osteogenic differentiation, cells were fixed in iced cold 70% ethanol and stained with Alizarin Red solution.

2.6. Reverse Transcription Polymerase Chain Reaction (RT-PCR). Cellular differentiation of rBM-MSCs towards mesodermal lineages was further confirmed with gene expression assay using RT-PCR. Total RNA of cells that were cultured in either normal medium or induction media (adipo and osteo) retrieved using TRIzol reagent kit (Invitrogen, USA). DNase treatment was carried out by adding 20.5 μ L RNA with

TABLE 3: PCR gene amplification conditions for GAPDH, osteopontin, osteonectin, PPAR γ , and C/EBPA gene for adipogenesis and osteogenesis differentiation assays.

Process	Temperature (°C)	Time	Cycle
Predenaturation	95	3 min	1
Denaturation	95	30 sec	35
Annealing		1 min	35
GAPDH	48.1		
Osteopontin	57.8		
Osteonectin	60.5		
PPAR γ	47.3		
C/EBPA	66.7		
Elongation	72	1 min	35
Final elongation	72	10 min	1
Incubation	10	∞	∞

2.5 μ L NE buffered DNase 1, 1 μ L of RNase inhibitor, and 1 μ L DNase 1 and incubated for 30 minutes at 37°C. Subsequently, 0.5 μ L of 0.25 M ethylene diamine tetraacetic acid (EDTA) was added and incubated for 10 minutes at 75°C. The RNA concentration was determined by using spectrophotometer. The cDNA was obtained by reverse transcription of 4 μ g of total RNA using 1 μ L oligo dT primer. Primers for PCR were adopted from the literature [16, 18, 40–42] as shown in Table 2. The detailed PCR procedures for cDNA were followed per Table 3.

2.7. Tritiated Thymidine Incorporation Assay. The proliferation of rBM-MSCs was determined by tritiated thymidine (3H-TdR) assay (Perkin Elmer, USA). The radioactive nucleotide 3H-TdR integrates only into actively proliferating cells during DNA synthesis, and the amount of 3H-TdR measured is directly proportional to the cell proliferation. Five thousand cells per well were cultured in 96-well plate for 24 h, 48 h, and 72 h. Cultures were pulsed with 10 μ L 3H-TdR (0.5 μ Ci/well) at 24 h prior to measurement. At the end of each time point (24 h, 48 h, and 72 h) cells were harvested onto glass filter mat (Perkin Elmer, USA) by using a 96-well plate automated cell harvester (Harvester Mach

III M, TOMTEC, USA). The filter mat was dried using oven (Penasonic, Malaysia) (120°C) for 10 min before adding 5 mL scintillation fluid (OptiPhase Supermix Cocktail; Perkin Elmer, USA). The filter mat was then sealed and fitted into a scintillation cassette for radioactive measurement using luminescent Microbeta counter (MicroBetaTrilux). Results were expressed as count per minute (CPM).

2.8. Growth Kinetic and Doubling Time. Growth kinetic of rBM-MSCs was performed using trypan blue exclusion test. Approximately, 150,000 cells were plated into 6-well plate. Cells were grown for 6 days with medium change which was performed at every 3 days. Cells were harvested every day and counted. Growth kinetic curves of rBM-MSCs from different passages were plotted. The initial seeding number, days in culture, and yield of MSC cultures were recorded and computed into doubling time. Doubling time was determined by Patterson Formula 1 and expressed as mean doubling time:

$$T_d = \frac{T \log 2}{\log(N_t/N_0)}, \quad (*)$$

where T_d is the doubling time (h), T is the time during which cells proliferated from N_0 to N_t (h), and N is the cell count.

2.9. Apoptosis Assay. Apoptosis assay was performed using Annexin V/Dead Cell Apoptosis kit with FITC conjugated Annexin V and PI (Invitrogen, USA). Annexin V is Ca^{2+} -dependent phospholipid binding protein that binds to phospholipid such as phosphatidylserine (PS). Annexin V along with propidium iodide (PI) allows identification of early apoptotic cells (PI negative; FITC Annexin V positive). Viable cells with intact membranes exclude PI, whereas membranes of dead and damage cells are permeable to PI [43]. Approximately 100,000 cells were washed with 1x Annexin binding buffer (ABB) and stained with 2 μ L Annexin V and 1 μ L PI for 15 min at room temperature. Cells were resuspended in 500 μ L 1xABB and acquired using LSR Fortessa flow cytometer (BD Bioscience, USA). For analysis, 10,000 cells were acquired and analysed using FACS Diva Software.

2.10. Senescence Associated β -Galactosidase (SA β -gal) Staining. Acid β -D-galactosidase is a hydrolase localized in lysosome which cleaves β -linked terminal galactosyl residues from substrates such as gangliosides, glycoproteins, and glycosaminoglycans [43]. Mammalian cells expressed lysosomal β -galactosidase (β -gal) activity at pH 4.0. Meanwhile, SA β -gal activity can be detected at pH 6 in senescence cells but not in proliferating cells. Both lysosomal β -gal and SA β -gal can be detected in situ by a cytochemical staining using chromogenic substrate 5-bromo-4-chloro-3-indolyl β -D-galactopyranoside (X-gal) [44]. X-gal cleaved by β -gal to produce insoluble blue precipitates [45]. Cells at passage two and passage five were fixed with 70% ethanol for 10 minutes and stained with X-gal in its respective buffer (pH 4 and pH 6) overnight before viewing under the phase contrast microscope. Senescent cells were evidenced by the formation of blue precipitate within the cells.

2.11. Cell Cycle Analysis. Cell cycle analysis of rBM-MSC was determined by measuring DNA content using PI dye. Cells at passage 2 and passage 5 were cultured in 25 cm² flasks. Upon reaching 80–90% confluency, cells were harvested and fixed with 70% ethanol and subjected to overnight incubation at –20°C. Fixed cells were washed with 1xPBS and incubated with 0.5 mL staining buffer which consisted of 100 μ g/mL PI (Molecular Probe, Invitrogen) and 20 ng/mL RNase (Sigma) in 1xPBS for 30 minutes. At least 10,000 cells were acquired by flow cytometer and analysed via ModFit LT software (Verity Software House, USA).

2.12. Statistical Analysis. Values for all measurements were presented as mean \pm SD unless otherwise stated. Comparison was performed by Student's *t*-test and one-way ANOVA. Significance levels were set at value $p \leq 0.05$.

3. Results

3.1. Optimization of rBM-MSC Culture. Upon in vitro culture, single cells of rat BM have started to form adherent cell colonies from day 3 onwards. The colony of spindle-shaped cells has profoundly increased in size at day 5 and day 7 (Figure 1(a)). To determine the optimal media for the growth of rBM-MSCs, several basal media and two concentrations of FBS were tested for the ability to support the growth of colony forming unit-fibroblast and cell expansion. Figure 1(b) shows the stained CFU-f of LDMEM, HDMEM, RPMI, and DMEM/F12 basal media supplemented with 10% FBS or 20% FBS, respectively. Regardless of the types of basal media, 20% supplemented FBS yields the highest number of colonies as compared to 10% FBS. Among all basal media, LDMEM reaps the highest number of colonies (CFU-f = 52), followed by DMEM/F12 (CFU-f = 26), RPMI (CFU-f = 24), and HDMEM (CFU-f = 12) (Figure 1(c)). To verify whether the number of colonies formed is accompanied by the total cell numbers, BM cells from passage 0 were cultured in respective basal media and serum concentrations. The number of expanding cells was calculated using trypan blue exclusion test at stipulated time points. As evidenced in CFU-f assay, the total cell counts are greater when 20% of FBS was consumed, whereas in terms of the type of basal medium, LDMEM induced a higher cell proliferation as compared to HDMEM, RPMI, and DMEM/F12 (Figure 1(d)).

3.2. Characterization of rBM-MSC. To analyse the expression of cell surface markers on rBM-MSCs, cells at passage 3 were subjected to the immunophenotyping. Flow cytometry result showed that rBM-MSCs are unequivocally positive for CD90.1 (94.8%), CD44H (41.6%), CD29 (99.7%), and CD71 (12.7%) and negative for hematopoietic markers CD45 (4.0%) and CD11b/c (4.3%) as shown in Figure 2(a). To assess the mesodermal differentiation ability of rBM-MSCs, cells at passage 3 were grown to the confluency and induced to differentiate into adipocytes and osteocytes using relevant induction media. Following 20 days of adipogenic induction, lipid vacuoles were detected by positive staining of Oil Red O whereas osteogenic differentiation was detected by

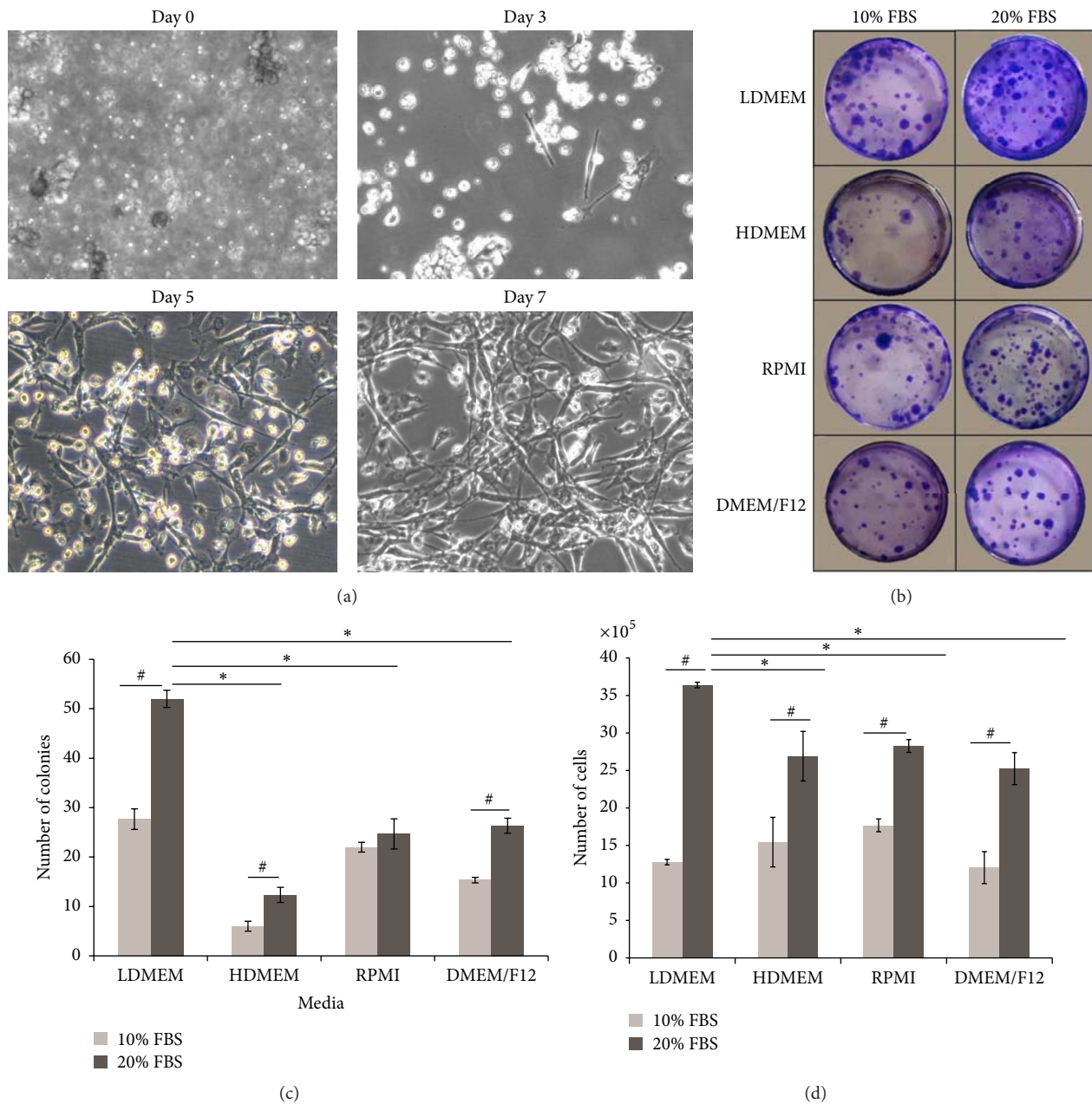


FIGURE 1: Generation and optimization of rBM-MSCs culture. Bone marrow was harvested from femur and tibia of SD rats and nucleated cells were cultured in T25 flask in day 0. By day 3, cells began to attach and heterogeneous population with predominant fibroblast-like morphology were observed by day 7 (a). One million of nucleated cells from bone marrow were cultured for 10 days in respective media and FBS concentrations. Colonies were subjected to crystal violet staining and colonies which brightly stained were counted (b). Four different basal media with 10% and 20% FBS concentration were utilized to culture 1×10^6 freshly isolated BM nucleated cells for CFU and proliferation assays. CFU-f and proliferation assays were measured using crystal violet staining and trypan blue exclusion test, respectively. Results were representative of three independent experiments. *Significant values were compared between LDMEM 20% and other basal media with 20% FBS; #significant values were compared between 10% FBS and 20% FBS of the respective media. $p \leq 0.05$. Microscopic magnification: 200x.

positive staining of Alizarin Red solution (Figure 2(b)). Cell cultured in expansion media (negative control) showed neither detectable lipid vacuoles nor calcium deposition. To further confirm the mesodermal differentiation, gene expression analysis of adipocytes and osteocytes specific

genes was conducted using RT-PCR. The selected adipocytes (PPAR γ and CEBP/A) and osteocytes gene (osteopontin and osteonectin) were analysed. Undifferentiated rBM-MSC (negative control) showed a faint expression of adipocytes and osteocytes genes. Differentiated rBM-MSCs (osteocytes

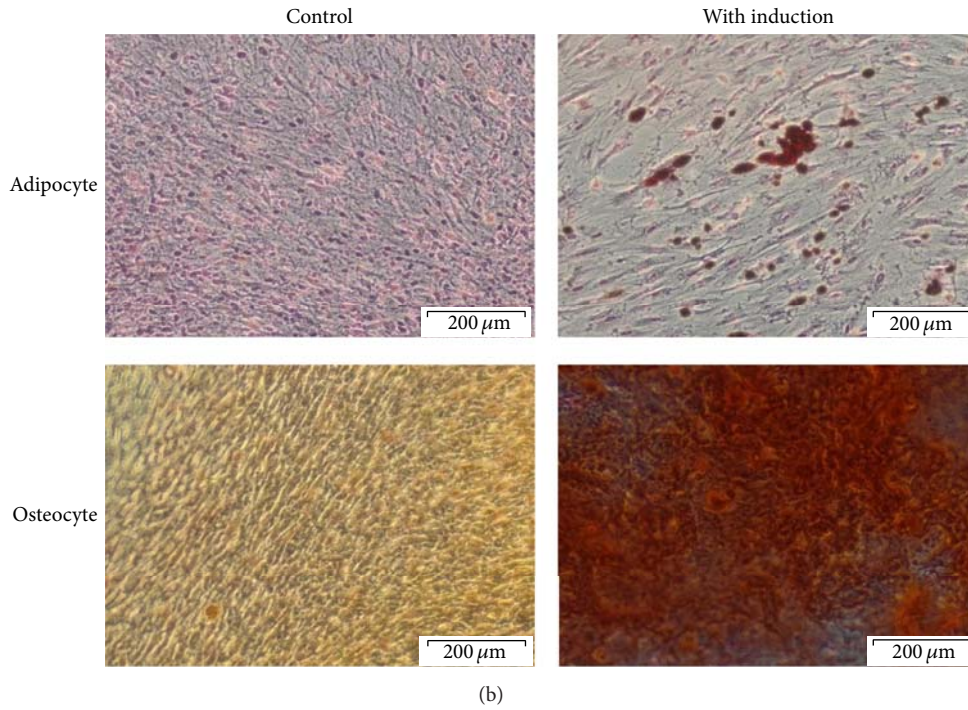
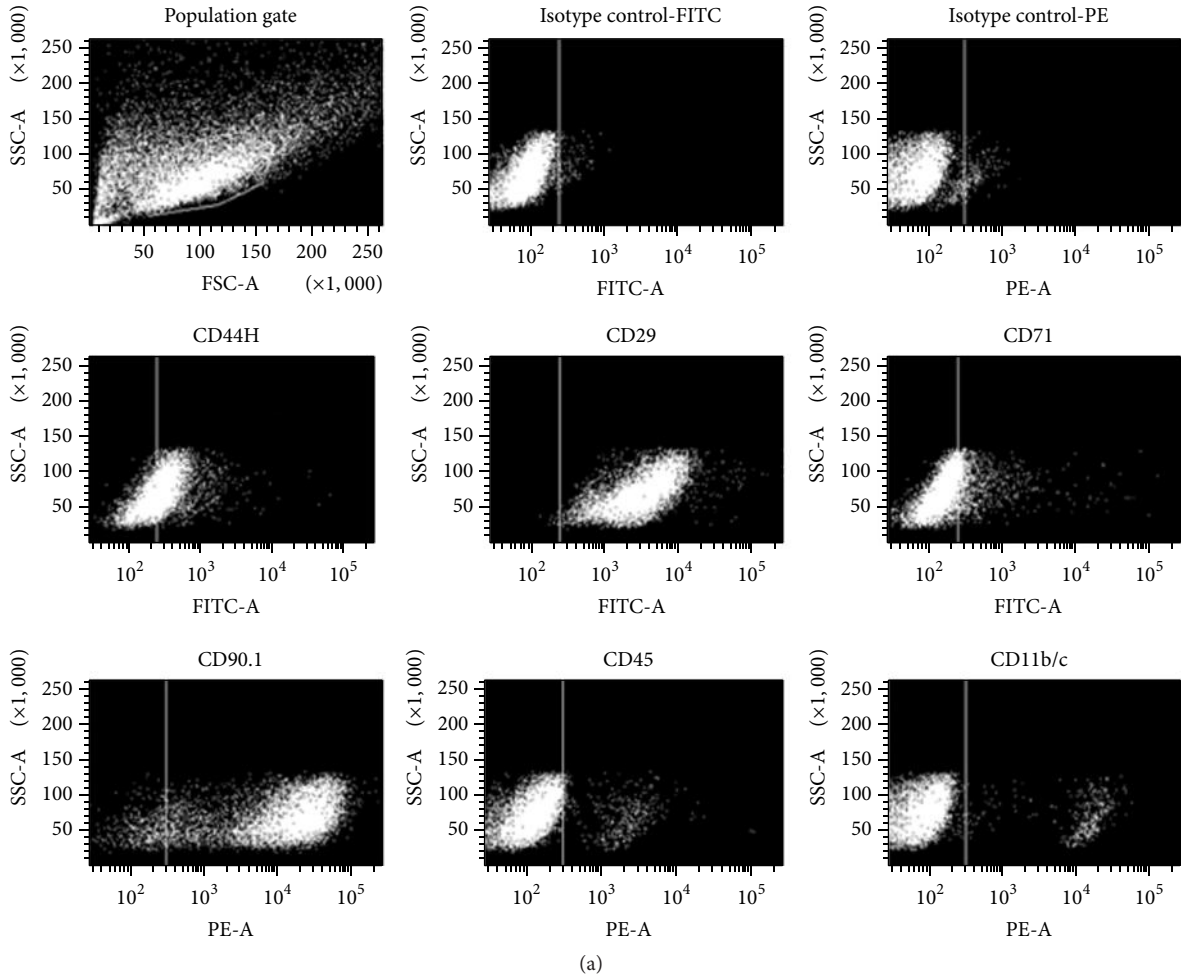


FIGURE 2: Continued.

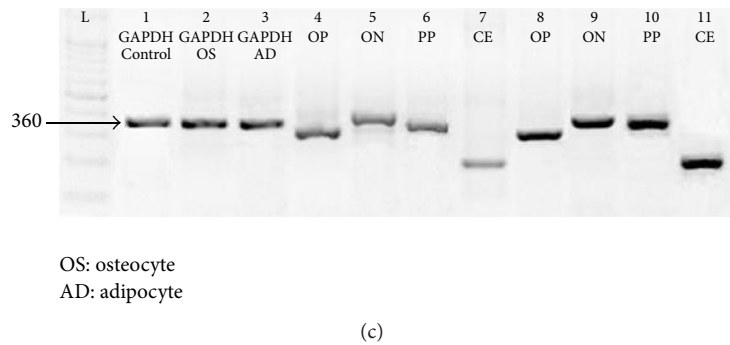


FIGURE 2: Characterization of rBM-MSCs. The immunophenotyping to characterize the surface markers was performed using rBM-MSC from passage 3. Cells were positively expressed as CD90.1, CD29, CD71, and CD44 and negatively expressed as CD11b/c and CD45 (a). Mesodermal differentiation was conducted using cells of passage 3 that is subjected to the relevant induction media. After 20 days of induction, cells were stained with Oil Red O solution and Alizarin Red solution, respectively. Adipogenic differentiation was evidenced by lipid droplet formation stained with Oil Red O whereas osteogenic differentiation was evidenced by calcium deposits stained with Alizarin Red (b). Gene expression of differentiated adipocytes and osteocytes was evaluated using RT-PCR. Untreated rBM-MSC (control) showed faint expression for osteocytes (c). Results were representative of 3 experiments. OP: osteopontin, ON: osteonectin, PP: PPAR γ , and CE: C/EBP α . Microscopic magnification: 200x.

and adipocytes) showed higher expression of adipocytes and osteocytes genes as compared to control as shown in Figure 2(c).

3.3. Growth Kinetics and Doubling Time of rBM-MSC. The growth pattern of rBM-MSCs was tracked by the morphological assessment, growth kinetics curve, and doubling time at various passages. The morphology of adherent cells appeared to be relatively smaller and defined at passage 1 till passage 3 (Figure 3(a)). It was noted that cells were assuming a uniform spindle shape till passage 3; however, the morphology has gradually changed from passage 4 onward into a more flatten, larger, and polygonal phenotypes. Although the growth curve of an individual cell passage from passages 1–5 had depicted an accepted sigmoid shape or exponential growth pattern, the duration of lag, log, and plateau phases is varied among numbers of passages (Figure 3(b)). Passages 1–3 cells reflected an initial lag phase for 1 day, followed by exponential log phase for 4 days and then a plateau phase. It was observed that passage 1 showed an abrupt log phase while other passages (P2-3) showed a gradual increase of log phase. However, the proliferative stage of log phase is not being spotted in cells from passages 4–5 which is an indication of growth arrest. The growth arrest of passages 4–5 rBM-MSCs was further confirmed with deduced doubling time. The doubling time of passages 1–3 rBM-MSCs is within 20–30 hours whereas passage 5 shows an extreme of 130 hours as shown in Figure 3(c).

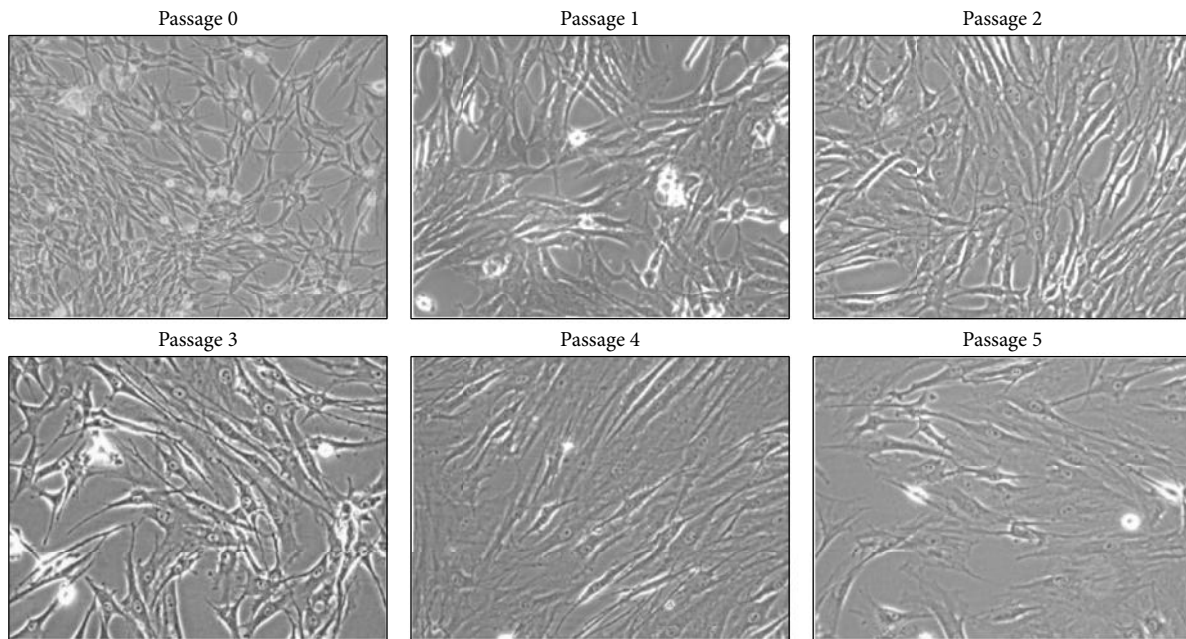
3.4. Rat Bone Marrow MSCs Undergo Cellular Senescence and Cell Cycle Arrest. Since rBM-MSCs from passages 1–5 exhibited various growth kinetic patterns with compromised log phases at late passages, another mean of measurement was opted to verify this phenomenon. The proliferation rate of rBM-MSCs was further rectified using tritiated thymidine (3H-Tdr) incorporation assay. The highest proliferation was

TABLE 4: Percentage of viability and early apoptosis at various passages of rBM-MSC.

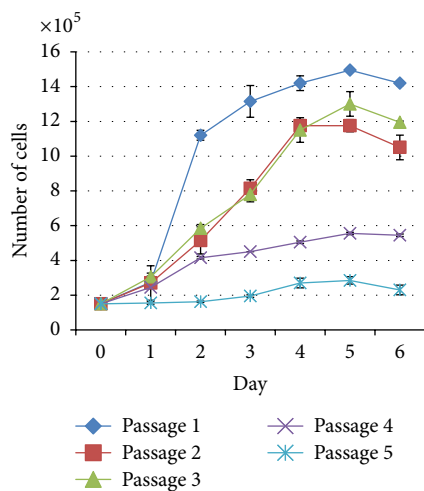
Passage	Viable cells (%)	Early apoptosis (%)
1	30.1 \pm 1.0	68.4 \pm 0.4
2	42.4 \pm 3.0	56.8 \pm 3.0
3	49.9 \pm 4.0	49.6 \pm 4.0
4	67.2 \pm 3.0	31.2 \pm 2.0
5	69.4 \pm 1.0	29.4 \pm 0.5

observed at 48 hours in all passages. However, the active proliferation was only noted at passages 1–3 while cell expansion was halted at passages 4–5 (Figure 4(a)). The complete halt in cell proliferation at passages 4–5 was further deciphered by the occurrence of senescence. When rBM-MSCs from passage 2 and passage 5 were stained with senescence marker, SA β -gal, only passage 5 rBM-MSCs were significantly positive for SA β -gal as evidence by blue precipitation within the cells while actively proliferating rBM-MSCs in passage 2 showed negative staining for β -gal (pH 6) (Figure 4(b)). To study the cell cycle pattern of rBM-MSC, DNA content of rBM-MSC at passage 2 and passage 5 was measured using PI staining. Result showed that almost all cells in passage 5 were arrested at G₀/G₁ phase (G₀/G₁ = 97.03%, S = 0.19%, and G₂/M = 2.78%) as compared to passage 2 (G₀/G₁ = 85.85%, S = 8.65%, and G₂/M = 5.5%) as shown in Figure 4(c).

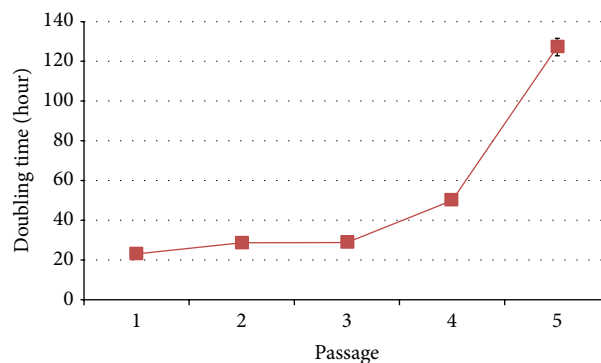
3.5. Senescence of rBM-MSCs Is Not Associated with Apoptosis Induction. Apoptosis assay was performed to assess the viability of rBM-MSCs at various passages (P1-P0) whether the documented cellular senescence is caused by the induction of apoptosis. The apoptosis results revealed that as the passage was increased the percentage of early apoptosis decreased while the percentage of viability is increased as shown in Table 4.



(a)



(b)



(c)

FIGURE 3: Growth kinetics and doubling time of rBM-MSC. Morphological observation of rBM-MSC cultured in LDMEM (20% FBS) in the presence of 20 ng/mL, 1% ITS, and 1% NEAA at various passages. Cells were successfully expanded until passage 5 and assumed a spindle-shaped fibroblast-like morphology. As the passage increased, polygonal and flatten shaped cells were predominating (a). Rat BM-MSCs were plated in 6-well plate at 150,000 cells/well, and media were changed every 2 days for 6 days. Cells depicted an initial lag phase for 1 day, followed by exponential log phase for 4 days, and then a plateau phase was observed (b). Doubling time was determined by Patterson Formula (*) and expressed as mean doubling time (c). The result represented the mean \pm SD. Microscopic magnification: 200x.

4. Discussion

Various studies have been conducted using animal models in attempt to evaluate the potential use of MSCs in clinical applications. As preclinical study is vital for clinical trials, this requires an establishment of animal-based MSCs culture system through a feasible isolation and expansion procedure at in vitro setting [15, 46, 47]. Several methods have been employed to isolate MSCs, mainly based on its plastic adherence property whereby whole bone marrow (BM) is

aspirated and directly plated into culture dish. This is the standard method of isolation that is mostly used in previous studies due to the cost effectiveness, straight forward, and less laborious nature of the procedures [48]. Besides plastic adherence, methods of refining MSC population such as density gradient separation technique [42, 49, 50] and enrichment of MSCs culture using magnetic cell sorting [51] were also tested widely. Previous studies have suggested that MSCs isolated from whole BM exhibited the superior cell growth in terms of absolute cell numbers, negligible hematopoietic

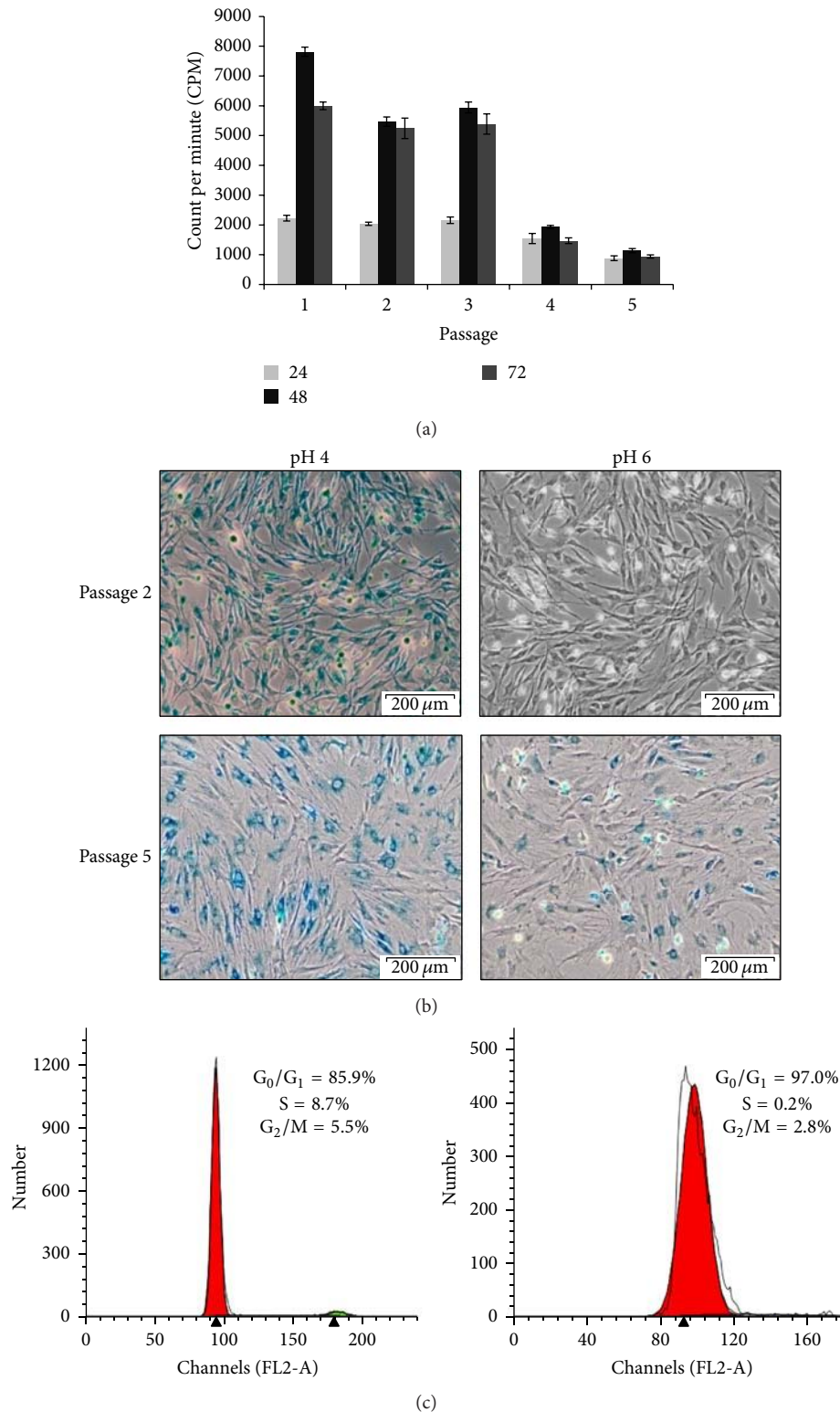


FIGURE 4: Cellular senescence and cell cycle arrest of culture expanded rBM-MSCs. Cells from passages 1–5 were seeded at 5000 cells/well cultured in 96-well plate for 24 h, 48 h, and 72 h. Cultures were pulsed with $10 \mu\text{L } ^3\text{H-TdR}$ at 24 hours prior to measurement. The rate of proliferation decreased as the passage increased (a). Cells at passage 2 and passage 5 were fixed with 70% ethanol for 10 minutes and stained with X-gal in the respective buffer overnight. Cells at passages 2 and 5 were stained positive with lysosomal β -gal (pH 4) staining showing that cells were expressing lysosomal β -gal in early passage as well as in late passage. Cells at passage 5 were stained positive for SA- β -gal (pH 6) staining as evidenced by blue precipitation but not at passage 2. Cells at passage 2 and passage 5 were cultured in 25 cm^2 flasks. Upon reaching 80%–90% confluency, cells were harvested and subjected to PI staining. Cells were analysed using flow cytometer. Results were representative of three independent experiments. Microscopic magnification: 200x.

contamination, higher CFU-f number, and a longer telomere length as compared to Percoll and Ficoll density separation techniques [50]. Hence, the present study has utilized a direct plating method of culturing whole BM from femur and tibia of Sprague Dawley rats.

The initial primary culture (P0) of BM was mixed with other cell populations which did not allow a clear discrimination between MSCs and other adherent cells. However, as the number of passages was increasing, the adherent cell culture became more morphologically homogenous. Along with MSCs, BM cultures at passage 0 were also found to be comprised of other primary BM cells such as macrophages and endothelial cells that promote heterogeneity of primary culture. Since the present study has utilized a whole BM, the contamination of other BM residing cells, namely, hematopoietic cells, fat cells, endothelial cells, and fibroblasts that may retain up to fewer passages of BM culture, could contribute to formation of mixed populations [52]. Nonetheless, mix populations of early bone marrow cells culture are crucial as the growth factors and multicellular interaction with other cells are needed for the initial colony forming and expansion of MSCs [53].

To date, there is no standard method for culturing rBM-MSCs. It is difficult to compare methods of culturing MSCs as there are high inconsistency among different laboratories such as choice of media, the type of serum, plating density, the addition of supplements, and level of confluency which play a crucial role in MSCs culture as it can affect the expansion, differentiation, and immunogenic properties of MSCs [50]. We have employed colony forming unit-fibroblast (CFU-f) assay to optimize the culture condition for rBM-MSC as this assay allows the identification of adherent cells with stem cell properties that expand to form colonies [42]. The current findings demonstrated that LDMEM basal medium with 20% FBS served as the optimal condition for rBM-MSCs expansion, yielding the highest CFU-f count. In line with this, Ayatollahi et al. (2012) had reported the excellent tropic effect of LDMEM basal medium to support and enhance the growth of MSCs as compared to the α MEM and HDMEM. Among all tested concentrations of FBS, 15% of supplemented FBS had shown a higher cell yield as compared to the lower concentrations, namely, 5% and 10% of FBS [54]. Since expanding rBM-MSCs from the primary culture are considered an arduous process and thus a higher concentration of FBS, 20% was opted and compared to the conventional 10% of FBS. As expected, 20% of FBS level has induced a higher number of colonies in all media as compared to 10% FBS (Figure 1). However, it is still unable to decipher whether the increased concentration of FBS has potentially slowed down the cellular senescence, although 20% FBS supplemented rBM-MSCs were expanded till passage 4/5 but the conventional FBS concentration fails to propagate cell number at very early passages.

High glucose DMEM and DMEM/f12 are among commonly used media for culturing adherent cells especially MSCs while RPMI are routinely used for culturing lymphocytes [46–60]. In this study, we have also consumed RPMI basal medium to culture rBM-MSC. In fact, rBM-MSCs were able to grow in RPMI although the CFU-f count was

lower than LDMEM. Overall, culture medium that contains HDMEM has contributed the lowest number of CFU-f as compared to LDMEM, DMEM/f12, and RPMI. Consumption of the basal medium that contains a high glucose level may jeopardise the beneficiary effects of culturing stem cells over a low glucose culture medium. It has been shown that culturing rat MSCs in high glucose medium is associated with cellular senescence while low glucose medium is enhancing proliferation and CFU counts while reducing the apoptosis [61]. Glucose is crucial source of cellular energy; however, the elevated concentration of glucose can raise the production of reactive oxygen species and thus leads to cell damage and cellular senescence [62]. Due to balanced oxidative stress in low glucose medium, stem cells might be stress-free and physiologically unchallenged since stem cells are very sensitive to the changes in the microenvironment.

Although the colonies formed in LDMEM culture medium are highest, further cultivation in the same medium with 20% FBS did not support the expansion of rBM-MSCs. This phenomenon is also observed in other basal media and thus prompted us to use additional growth factors. Basic FGF was used to enhance the growth of rBM-MSCs in our study as it is the most common growth factor that is known to induce proliferation of MSCs [63–66]. To further improve rBM-MSC growth, 1% ITS and 1% NEAA were also added in culture along with 20 ng/mL bFGF. The addition of bFGF and supplements significantly altered the cell size and appearance of rBM-MSC as compared to rBM-MSC cultured without any supplements (data not shown). It is well established that MSCs at in vitro culture contain two distinct types of morphologies: (1) small spindle-shaped fibroblast-like cells which proliferate rapidly and (2) large flattened cells with slower proliferation rate [16, 46, 50, 57]. Similar to what has been reported, rBM-MSCs cultured in optimized medium and supplements appeared as spindle-shaped and fibroblast-like but when the number of passages increased, a gradual domination of large and flattened cells was noted. Similar observations were also reported by previous studies whereby the number of large and flat cells increased over the time in cultures [49, 57]. This transition could be due to losing of cell integrity and also loss of autocrine and paracrine effects, resulting in inadequate formation of microenvironment that is necessary for MSCs proliferation. Furthermore, it could also be due to an autocommitment of MSCs towards mature mesodermal lineages. Based on RT-PCR data, it has been shown that MSCs at resting condition without inductive media are slightly expressed RNAs that lead to adipogenic and osteogenic differentiation. This could be accountable for the slow growth rate of MSCs during the expansion period where culture-driven cellular commitment towards mature cells reduces the self-renewal and propagation of stem cell population.

Mesenchymal stem cells characterization mainly relies on the assessment of (1) surface antigen markers expression and (2) the ability of MSC to differentiate into mesodermal lineages (osteocytes, adipocytes, and chondrocytes). To date, there are no specific markers for MSCs; thus a combination of commonly accepted positive and negative markers was opted for the MSC's immunophenotyping. We have shown

that rBM-MSCs were positive for CD29, CD90.1, CD44H, and CD71 and negative for hematopoietic markers CD45 and CD11b/c [15, 42, 48, 54, 65]. Upon induction, rBM-MSCs were able to differentiate into adipocytes and osteocytes, and this finding was further confirmed by expression of osteocytes (osteopontin and osteonectin) and adipocytes (PPAR γ and CEBP/A) genes. Interestingly, rBM-MSCs without the induction medium also expressed a low level of these genes. Others have also reported similar findings where the positive expression of osteonectin and osteopontin and expression of adipogenic gene (PPAR γ) were detected in MSCs in the absence of induction medium [16, 67]. The expression of adipogenic and osteogenic genes in undifferentiated rBM-MSCs might be the reason why the cells easily reach senescence and can readily differentiate into mesenchymal stem cells' own mesodermal lineages.

To determine the proliferative capacity of rBM-MSCs, tritiated thymidine (3H-TdR) and growth kinetic assays were performed. Rat BM-MSCs were spotted to proliferate rapidly at passage 1 until passage 3 while reduction in proliferation was evidenced at passage 3 onwards and almost ceased at passage 5. These results were further confirmed with 3H-TdR assay and deduced doubling time. Cells at passages 1–3 had maintained a stable doubling time (30 hrs); however, the doubling time was started to upraise at passage 4 (50 hrs) and reached maximum at passage 5 (130 hrs). However, the cells were unable to be further expanded beyond passage 5 due to the complete halt in cell growth despite the use of optimized culture medium. This observation is not a new phenomenon as Liu et al. (2003) also reported a similar finding that rBM-MSCs from Wister rats were only being cultured till 4 successful passages [49].

The ceased proliferation of passage 5 rBM-MSCs has triggered the need for further exploration of the possibility of apoptosis or senescence. The apoptosis result was not in agreement with the spotted growth arrest of passage 4–5 cells. Surprisingly, the viability of cells was improved with the number of passages. However, a substantial fraction of cells at all passages was undergoing early apoptosis process but not late apoptosis as shown in Table 4. The expression of higher early apoptosis in P1–3 cells was accompanied by neither progression towards late apoptosis nor cell death. However, it could be possible that those cells in early apoptosis are able to recover as the translocation of PS was reversible in apoptosis induced by tumour suppressor protein p53 provided the apoptosis stimuli were removed [68].

Our data also revealed that rBM-MSCs almost cease to proliferate at passage 5 and morphology of cells was large and flattened which are characteristics of cellular senescence. β -gal is found in lysosomes of all types of cells at all stages including proliferating, quiescent, and senescence cells and can be detected by X-gal staining at pH 4 [44]. Meanwhile, SA β -gal staining is detectable at pH 6.0 and expressed by cells that undergo senescence but not in actively proliferating cells [44, 69]. Result of X-gal staining on passage 2 and passage 5 rBM-MSC showed a positive staining for senescence in passage 5 rBM-MSCs but not in passage 2. Lysosomal β -gal assay was also performed on rBM-MSC in passage 2 and passage 5 and our finding showed positive staining for

lysosomal β -gal. However, since MSCs almost ceased in proliferation as indicated in Figure 3, we were unable to further passage the MSCs and explore the senescence in later passages.

The hallmark of senescence is the inability of cells to advance into cell cycle. Senescence cells show growth arrest at G₁ phase of cell cycle, despite sufficient growth condition, cells still fail to initiate DNA replication [70]. Cells at passage 5 were mainly arrested at G₀/G₁ phase of cell cycle. On the other hand, rBM-MSCs at passage 2 stained which is negative for SA β -gal showing a progression in cell cycle with higher percentage of S and G₂/M phase as compared to passage 5. The reduced proliferation, changes in morphology from spindle-shape fibroblast-like cells into large flattened cells, positive staining for SA β -gal, and growth arrest of rBM-MSC passage 5 at G₀/G₁ phase of cell cycle could be an evidence of cells undergoing senescence.

Study on human fibroblasts demonstrated that, under an inadequate culture condition (0.25% FBS), the cells underwent a premature growth arrest. When fibroblasts were initially expanded in 10% FBS and later grown in 0.25% FBS, they showed a substantial arrest in cellular growth. However, the cell growth recovered and cell cycle machinery was activated when the culture was reconstituted with 10% FBS. In fact, transfection of HTERT (human telomerase reverse transcriptase) as well did not abolish the growth retardation in the presence of 0.25% of FBS [71]. Regardless of the elongation of telomerase length, serum deprivation elevated p16^{INK4a}, a tumour suppressor protein that inhibits cyclin-dependent kinases (CDKs) and leads to a permanent growth arrest [72]. Similarly, human MSCs that underwent a premature growth arrest during the in vitro culture as well showed a significant change in p16^{INK4a} level [73]. It was elegantly shown that the suppression of p16^{INK4a} in human MSCs by wild-type p53 inducible phosphatase-1 (Wip-1), a stress modulator, extended the life-span of human MSCs while maintaining its multipotent differentiation potential [73].

In conclusion, the present study has successfully generated and characterized the rBM-MSCs from SD rats with optimized culture conditions based on the choice of basal medium, concentration of FBS, and growth factor supplements. The basal media LDMEM and 20% FBS provide the optimal culture condition for expanding rBM-MSC and the addition of bFGF, ITS, and NEAA significantly enhanced the morphology and proliferation capacity of rBM-MSCs at very early passages. Under the in vitro culture condition, even with optimized culture conditions, rBM-MSCs were undergoing cellular senescence which may relate to the gradual autocommitment of rBM-MSC into mature cells. Thus, further research is necessary to understand the internal and external cues that trigger the process of senescence in culture expanded rBM-MSCs.

Competing Interests

The authors declare that there are no competing interests regarding the publication of this paper and regarding the funding that they have received.

Acknowledgments

This research work is supported by Fundamental Research Grant Scheme (FRGS), 04-01-12-1131FR, and Research University Grant Scheme (RUGS) 04-02-12-1757RU.

References

- [1] A. J. Friedenstein, R. K. Chailakhjan, and K. S. Lalykina, "The development of fibroblast colonies in monolayer cultures of guinea-pig bone marrow and spleen cells," *Cell Proliferation*, vol. 3, no. 4, pp. 393–403, 1970.
- [2] M. F. Pittenger, A. M. Mackay, S. C. Beck et al., "Multilineage potential of adult human mesenchymal stem cells," *Science*, vol. 284, no. 5411, pp. 143–147, 1999.
- [3] M. C. Stewart and A. A. Stewart, "Mesenchymal stem cells: characteristics, sources, and mechanisms of action," *Veterinary Clinics of North America: Equine Practice*, vol. 27, no. 2, pp. 243–261, 2011.
- [4] C.-D. Wan, R. Cheng, H.-B. Wang, and T. Liu, "Immunomodulatory effects of mesenchymal stem cells derived from adipose tissues in a rat orthotopic liver transplantation model," *Hepatobiliary and Pancreatic Diseases International*, vol. 7, no. 1, pp. 29–33, 2008.
- [5] M. Giuliani, M. Fleury, A. Vernochet et al., "Long-lasting inhibitory effects of fetal liver mesenchymal stem cells on T-lymphocyte proliferation," *PLoS ONE*, vol. 6, no. 5, Article ID e19988, 2011.
- [6] H. E. Young, T. A. Steele, R. A. Bray et al., "Human reserve pluripotent mesenchymal stem cells are present in the connective tissues of skeletal muscle and dermis derived from fetal, adult, and geriatric donors," *The Anatomical Record*, vol. 264, no. 1, pp. 51–62, 2001.
- [7] L.-L. Lu, Y.-J. Liu, S.-G. Yang et al., "Isolation and characterization of human umbilical cord mesenchymal stem cells with hematopoiesis-supportive function and other potentials," *Haematologica*, vol. 91, no. 8, pp. 1017–1026, 2006.
- [8] O. K. Lee, T. K. Kuo, W.-M. Chen, K.-D. Lee, S.-L. Hsieh, and T.-H. Chen, "Isolation of multipotent mesenchymal stem cells from umbilical cord blood," *Blood*, vol. 103, no. 5, pp. 1669–1675, 2004.
- [9] T. C. Tran, K. Kimura, M. Nagano et al., "Identification of human placenta-derived mesenchymal stem cells involved in re-endothelialization," *Journal of Cellular Physiology*, vol. 226, no. 1, pp. 224–235, 2011.
- [10] A. Nimura, T. Muneta, H. Koga et al., "Increased proliferation of human synovial mesenchymal stem cells with autologous human serum: comparisons with bone marrow mesenchymal stem cells and with fetal bovine serum," *Arthritis and Rheumatism*, vol. 58, no. 2, pp. 501–510, 2008.
- [11] K. Bieback, S. Kern, H. Klüter, and H. Eichler, "Critical parameters for the isolation of mesenchymal stem cells from umbilical cord blood," *STEM CELLS*, vol. 22, no. 4, pp. 625–634, 2004.
- [12] A. Peister, J. A. Mellad, B. L. Larson, B. M. Hall, L. F. Gibson, and D. J. Prockop, "Adult stem cells from bone marrow (MSCs) isolated from different strains of inbred mice vary in surface epitopes, rates of proliferation, and differentiation potential," *Blood*, vol. 103, no. 5, pp. 1662–1668, 2004.
- [13] G. Ren, J. Su, L. Zhang et al., "Species variation in the mechanisms of mesenchymal stem cell-mediated immunosuppression," *Stem Cells*, vol. 27, no. 8, pp. 1954–1962, 2009.
- [14] S. M. Devine, A. M. Bartholomew, N. Mahmud et al., "Mesenchymal stem cells are capable of homing to the bone marrow of non-human primates following systemic infusion," *Experimental Hematology*, vol. 29, no. 2, pp. 244–255, 2001.
- [15] E. H. Javazon, D. C. Colter, E. J. Schwarz, and D. J. Prockop, "Rat marrow stromal cells are more sensitive to plating density and expand more rapidly from single-cell-derived colonies than human marrow stromal cells," *STEM CELLS*, vol. 19, no. 3, pp. 219–225, 2001.
- [16] E. Karaoz, A. Aksoy, S. Ayhan, A. E. SarIboyaçI, F. Kaymaz, and M. Kasap, "Characterization of mesenchymal stem cells from rat bone marrow: ultrastructural properties, differentiation potential and immunophenotypic markers," *Histochemistry and Cell Biology*, vol. 132, no. 5, pp. 533–546, 2009.
- [17] B. Johnstone, T. M. Hering, A. I. Caplan, V. M. Goldberg, and J. U. Yoo, "In vitro chondrogenesis of bone marrow-derived mesenchymal progenitor cells," *Experimental Cell Research*, vol. 238, no. 1, pp. 265–272, 1998.
- [18] M. B. Eslaminejad, S. Mardpour, and M. Ebrahimi, "Mesenchymal stem cells derived from rat epicardial versus epididymal adipose tissue," *Iranian Journal of Basic Medical Sciences*, vol. 14, no. 1, pp. 25–34, 2011.
- [19] D. R. Martin, N. R. Cox, T. L. Hathcock, G. P. Niemeyer, and H. J. Baker, "Isolation and characterization of multipotential mesenchymal stem cells from feline bone marrow," *Experimental Hematology*, vol. 30, no. 8, pp. 879–886, 2002.
- [20] S. Violini, P. Ramelli, L. F. Pisani, C. Gorni, and P. Mariani, "Horse bone marrow mesenchymal stem cells express embryo stem cell markers and show the ability for tenogenic differentiation by in vitro exposure to BMP-12," *BMC Cell Biology*, vol. 10, article 29, 2009.
- [21] Q.-P. Xie, H. Huang, B. Xu et al., "Human bone marrow mesenchymal stem cells differentiate into insulin-producing cells upon microenvironmental manipulation in vitro," *Differentiation*, vol. 77, no. 5, pp. 483–491, 2009.
- [22] S. H. Hong, E. J. Gang, J. A. Jeong et al., "In vitro differentiation of human umbilical cord blood-derived mesenchymal stem cells into hepatocyte-like cells," *Biochemical and Biophysical Research Communications*, vol. 330, no. 4, pp. 1153–1161, 2005.
- [23] W. Xu, X. Zhang, H. Qian et al., "Mesenchymal stem cells from adult human bone marrow differentiate into a cardiomyocyte phenotype in vitro," *Experimental Biology and Medicine*, vol. 229, no. 7, pp. 623–631, 2004.
- [24] E. J. Gang, J. A. Jeong, S. H. Hong et al., "Skeletal myogenic differentiation of mesenchymal stem cells isolated from human umbilical cord blood," *STEM CELLS*, vol. 22, no. 4, pp. 617–624, 2004.
- [25] L. Hou, H. Cao, D. Wang et al., "Induction of umbilical cord blood mesenchymal stem cells into neuron-like cells in vitro," *International Journal of Hematology*, vol. 78, no. 3, pp. 256–261, 2003.
- [26] J. Oswald, S. Boxberger, B. Jørgensen et al., "Mesenchymal stem cells can be differentiated into endothelial cells in vitro," *STEM CELLS*, vol. 22, no. 3, pp. 377–384, 2004.
- [27] J.-H. Kim, Y.-S. Kim, K. Park et al., "Antitumor efficacy of cisplatin-loaded glycol chitosan nanoparticles in tumor-bearing mice," *Journal of Controlled Release*, vol. 127, no. 1, pp. 41–49, 2008.
- [28] K. Guo, J. P. Tang, L. Jie et al., "Engineering the first chimeric antibody in targeting intracellular PRL-3 oncoprotein for cancer therapy in mice," *Oncotarget*, vol. 3, no. 2, pp. 158–171, 2012.

- [29] S. D. Kobayashi, N. Malachowa, A. R. Whitney et al., "Comparative analysis of USA300 virulence determinants in a rabbit model of skin and soft tissue infection," *Journal of Infectious Diseases*, vol. 204, no. 6, pp. 937–941, 2011.
- [30] S. J. Ferng, D. E. Gonzalez, M. N. Nguyen, S. J. Sherman, T. Falk, and H. L. Rilo, "Evaluation of a Parkinson's disease model in medaka fish," *The FASEB Journal*, vol. 27, no. 1, supplement, p. 567.1, 2013.
- [31] N. Tajiri, T. Yasuhara, T. Shingo et al., "Exercise exerts neuroprotective effects on Parkinson's disease model of rats," *Brain Research*, vol. 1310, pp. 200–207, 2010.
- [32] L. Fairbairn, R. Kapetanovic, D. P. Sester, and D. A. Hume, "The mononuclear phagocyte system of the pig as a model for understanding human innate immunity and disease," *Journal of Leukocyte Biology*, vol. 89, no. 6, pp. 855–871, 2011.
- [33] J. Kocerha, Yuhong Liu, Kate Nelson et al., "Noncoding RNA dysregulation in a longitudinal study of peripheral blood from a transgenic Huntington's disease monkey model," in *Proceedings of the Society for Neuroscience Conference*, 2012.
- [34] I. Sekiya, B. L. Larson, J. R. Smith, R. Pochampally, J.-G. Cui, and D. J. Prockop, "Expansion of human adult stem cells from bone marrow stroma: conditions that maximize the yields of early progenitors and evaluate their quality," *Stem Cells*, vol. 20, no. 6, pp. 530–541, 2002.
- [35] Z. Qu-Petersen, B. Deasy, R. Jankowski et al., "Identification of a novel population of muscle stem cells in mice: potential for muscle regeneration," *The Journal of Cell Biology*, vol. 157, no. 5, pp. 851–864, 2002.
- [36] D. J. Simmons, P. Seitz, L. Kidder et al., "Partial characterization of rat marrow stromal cells," *Calcified Tissue International*, vol. 48, no. 5, pp. 326–334, 1991.
- [37] J. E. Aubin, "Osteoprogenitor cell frequency in rat bone marrow stromal populations: role for heterotypic cell-cell interactions in osteoblast differentiation," *Journal of Cellular Biochemistry*, vol. 72, no. 3, pp. 396–410, 1999.
- [38] L. K. Chelluri, R. Kancharla, N. Turlapati et al., "Improved differentiation protocol of rat bone marrow precursors to functional islet like cells," *Stem Cell Studies*, vol. 1, no. 1, article e5, 2011.
- [39] Z. Neshati, M. M. Matin, A. R. Bahrami, and A. Moghimi, "Differentiation of mesenchymal stem cells to insulin-producing cells and their impact on type 1 diabetic rats," *Journal of Physiology and Biochemistry*, vol. 66, no. 2, pp. 181–187, 2010.
- [40] M. Sgodda, H. Aurich, S. Kleist et al., "Hepatocyte differentiation of mesenchymal stem cells from rat peritoneal adipose tissue *in vitro* and *in vivo*," *Experimental Cell Research*, vol. 313, no. 13, pp. 2875–2886, 2007.
- [41] Y.-C. Shang, S.-H. Wang, F. Xiong et al., "Wnt3a signaling promotes proliferation, myogenic differentiation, and migration of rat bone marrow mesenchymal stem cells," *Acta Pharmacologica Sinica*, vol. 28, no. 11, pp. 1761–1774, 2007.
- [42] H. Yoshimura, T. Muneta, A. Nimura, A. Yokoyama, H. Koga, and I. Sekiya, "Comparison of rat mesenchymal stem cells derived from bone marrow, synovium, periosteum, adipose tissue, and muscle," *Cell and Tissue Research*, vol. 327, no. 3, pp. 449–462, 2007.
- [43] D. J. Kurz, S. Decary, Y. Hong, and J. D. Erusalimsky, "Senescence-associated β -galactosidase reflects an increase in lysosomal mass during replicative ageing of human endothelial cells," *Journal of Cell Science*, vol. 113, no. 20, pp. 3613–3622, 2000.
- [44] G. P. Dimri, X. Lee, G. Basile et al., "A biomarker that identifies senescent human cells in culture and in aging skin *in vivo*," *Proceedings of the National Academy of Sciences of the United States of America*, vol. 92, no. 20, pp. 9363–9367, 1995.
- [45] J. P. Horwitz, J. Chua, R. J. Curby et al., "Substrates for cytochemical demonstration of enzyme activity. I. Some substituted 3-indolyl-12-D-glycopyranosides," *Journal of Medicinal Chemistry*, vol. 7, no. 4, pp. 574–575, 1964.
- [46] D. C. Colter, I. Sekiya, and D. J. Prockop, "Identification of a subpopulation of rapidly self-renewing and multipotential adult stem cells in colonies of human marrow stromal cells," *Proceedings of the National Academy of Sciences of the United States of America*, vol. 98, no. 14, pp. 7841–7845, 2001.
- [47] G. Fan, L. Wen, M. Li et al., "Isolation of mouse mesenchymal stem cells with normal ploidy from bone marrows by reducing oxidative stress in combination with extracellular matrix," *BMC Cell Biology*, vol. 12, no. 1, article 30, 2011.
- [48] E. Karaöz, A. Okçu, G. Gacar, Ö. Sağlam, S. Yürüker, and H. Kenar, "A comprehensive characterization study of human bone marrow mscs with an emphasis on molecular and ultrastructural properties," *Journal of Cellular Physiology*, vol. 226, no. 5, pp. 1367–1382, 2011.
- [49] Y. Liu, J. Song, W. Liu, Y. Wan, X. Chen, and C. Hu, "Growth and differentiation of rat bone marrow stromal cells: does 5-azacytidine trigger their cardiomyogenic differentiation?" *Cardiovascular Research*, vol. 58, no. 2, pp. 460–468, 2003.
- [50] K. Mareschi, D. Rustichelli, R. Calabrese et al., "Multipotent mesenchymal stromal stem cell expansion by plating whole bone marrow at a low cellular density: a more advantageous method for clinical use," *Stem Cells International*, vol. 2012, Article ID 920581, 10 pages, 2012.
- [51] L. Zhang and C. Chan, "Isolation and enrichment of rat mesenchymal stem cells (MSCs) and separation of single-colony derived MSCs," *Journal of Visualized Experiments*, no. 37, 2010.
- [52] H. Castro-Malaspina, R. E. Gay, G. Resnick et al., "Characterization of human bone marrow fibroblast colony-forming cells (CFU-F) and their progeny," *Blood*, vol. 56, no. 2, pp. 289–301, 1980.
- [53] S. Nadri, M. Soleimani, R. H. Hossenli, M. Massumi, A. Atashi, and R. Izadpanah, "An efficient method for isolation of murine bone marrow mesenchymal stem cells," *International Journal of Developmental Biology*, vol. 51, no. 8, pp. 723–729, 2007.
- [54] M. Ayatollahi, M. K. Salmani, B. Geramizadeh, S. Z. Tabei, M. Soleimani, and M. H. Sanati, "Conditions to improve expansion of human mesenchymal stem cells based on rat samples," *World Journal of Stem Cells*, vol. 4, no. 1, pp. 1–8, 2012.
- [55] A. Bartholomew, C. Sturgeon, M. Siatskas et al., "Mesenchymal stem cells suppress lymphocyte proliferation *in vitro* and prolong skin graft survival *in vivo*," *Experimental Hematology*, vol. 30, no. 1, pp. 42–48, 2002.
- [56] T. Deuse, M. Stubbendorff, K. Tang-Quan et al., "Immunogenicity and immunomodulatory properties of umbilical cord lining mesenchymal stem cells," *Cell Transplantation*, vol. 20, no. 5, pp. 655–667, 2011.
- [57] B. Neuhuber, S. A. Swanger, L. Howard, A. Mackay, and I. Fischer, "Effects of plating density and culture time on bone marrow stromal cell characteristics," *Experimental Hematology*, vol. 36, no. 9, pp. 1176–1185, 2008.
- [58] P. A. Sotiropoulou, S. A. Perez, M. Salagianni, C. N. Baxevanis, and M. Papamichail, "Characterization of the optimal culture

- conditions for clinical scale production of human mesenchymal stem cells," *Stem Cells*, vol. 24, no. 2, pp. 462–471, 2006.
- [59] R. Ramasamy, C. K. Tong, W. K. Yip, S. Vellasamy, B. C. Tan, and H. F. Seow, "Basic fibroblast growth factor modulates cell cycle of human umbilical cord-derived mesenchymal stem cells," *Cell Proliferation*, vol. 45, no. 2, pp. 132–139, 2012.
- [60] M. Krampera, S. Glennie, J. Dyson et al., "Bone marrow mesenchymal stem cells inhibit the response of naive and memory antigen-specific T cells to their cognate peptide," *Blood*, vol. 101, no. 9, pp. 3722–3729, 2003.
- [61] A. Stolzing, N. Coleman, and A. Scutt, "Glucose-induced replicative senescence in mesenchymal stem cells," *Rejuvenation Research*, vol. 9, no. 1, pp. 31–35, 2006.
- [62] T.-C. Chang, M.-F. Hsu, and K. K. Wu, "High glucose stress induces mesenchymal stromal cell senescence through up-regulating autophagy (LB842)," *The FASEB Journal*, vol. 28, no. 1, supplement LB842, 2014.
- [63] S. Tsutsumi, A. Shimazu, K. Miyazaki et al., "Retention of multilineage differentiation potential of mesenchymal cells during proliferation in response to FGF," *Biochemical and Biophysical Research Communications*, vol. 288, no. 2, pp. 413–419, 2001.
- [64] K. Hanada, J. E. Dennis, and A. I. Caplan, "Stimulatory effects of basic fibroblast growth factor and bone morphogenetic protein-2 on osteogenic differentiation of rat bone marrow-derived mesenchymal stem cells," *Journal of Bone and Mineral Research*, vol. 12, no. 10, pp. 1606–1614, 1997.
- [65] U. Nekanti, L. Mohanty, P. Venugopal, S. Balasubramanian, S. Totey, and M. Ta, "Optimization and scale-up of Wharton's jelly-derived mesenchymal stem cells for clinical applications," *Stem Cell Research*, vol. 5, no. 3, pp. 244–254, 2010.
- [66] L.-E. Zaragosi, G. Ailhaud, and C. Dani, "Autocrine fibroblast growth factor 2 signaling is critical for self-renewal of human multipotent adipose-derived stem cells," *Stem Cells*, vol. 24, no. 11, pp. 2412–2419, 2006.
- [67] L. Peng, Z. Jia, X. Yin et al., "Comparative analysis of mesenchymal stem cells from bone marrow, cartilage, and adipose tissue," *Stem Cells and Development*, vol. 17, no. 4, pp. 761–773, 2008.
- [68] F. J. Geske, R. Lieberman, R. Strange, and L. E. Gerschenson, "Early stages of p53-induced apoptosis are reversible," *Cell Death and Differentiation*, vol. 8, no. 2, pp. 182–191, 2001.
- [69] B. Van Der Loo, M. J. Fenton, and J. D. Erusalimsky, "Cytological detection of a senescence-associated β -galactosidase in endothelial and smooth muscle cells from human and rabbit blood vessels," *Experimental Cell Research*, vol. 241, no. 2, pp. 309–315, 1998.
- [70] J. Campisi and F. D'Adda Di Fagagna, "Cellular senescence: when bad things happen to good cells," *Nature Reviews Molecular Cell Biology*, vol. 8, no. 9, pp. 729–740, 2007.
- [71] R. D. Ramirez, C. P. Morales, B.-S. Herbert et al., "Putative telomere-independent mechanisms of replicative aging reflect inadequate growth conditions," *Genes and Development*, vol. 15, no. 4, pp. 398–403, 2001.
- [72] M. Serrano, A. W. Lin, M. E. McCurrach, D. Beach, and S. W. Lowe, "Oncogenic ras provokes premature cell senescence associated with accumulation of p53 and p16^{INK4a}," *Cell*, vol. 88, no. 5, pp. 593–602, 1997.
- [73] J.-S. Lee, M.-O. Lee, B.-H. Moon, S. H. Shim, A. J. Fornace Jr., and H.-J. Cha, "Senescent growth arrest in mesenchymal stem cells is bypassed by Wip1-mediated downregulation of intrinsic stress signaling pathways," *STEM CELLS*, vol. 27, no. 8, pp. 1963–1975, 2009.